

FIVE-LEVEL SVM INVERTER FOR AN INDUCTION MOTOR WITH DIRECT TORQUE CONTROLLER

O.Chandra sekhar¹ K.Chandra sekhar²

E.E.E Department, Vignan's Lara Institute of Technology and Science, Vadlamudi, Guntur, India Sekhar.obbu@gmail.com

²E.E.E Department, R.V.R & J.C College of Engg, Chowdavaram, Guntur, India, cskoritala@gmail.com

Abstract: *The Direct Torque Control (DTC) is very good control scheme for dynamic performance and it is easy to implement and decoupling of motor variables along rotor flux axis is not required. The proposed DTC scheme uses the fundamental stator voltage vector for identification of sector for selection switching of vector to control stator flux and the torque. In this paper DTC proposed using five-level inverter has 125 space vector switching states and there are 61 effective vectors are possible. The proposed scheme is capable for enough degrees of freedom to control both electromagnetic torque and stator flux with very low ripple. From the simulation results shows that feeding electrical drive with five-level inverter can greatly improves the drive performance as compared to the 2 and 3-level inverters. The performance of this control method has been demonstrated by simulations performed using a versatile simulation package, Matlab/Simulink.*

Key words: DTC, Five-level inverter, Space vector modulation.

1. Introduction

These days, there is an increasing demand for inverter-fed Induction Motor (IM) drive with good performance. IM drive is used in various applications such as electric vehicles, ventilation systems for large buildings and for industrial drives with variable speed requirements. They are also used for pump, elevator, conveyor and machine tool drives. These applications require frequent torque control to control speed of vehicle. This has resulted in the need of control scheme with high performance, fast transient and accurate control of torque for induction motor drive. There are mainly two schemes used for these applications. One is vector control and the other is the DTC [1], [2]. The DTC gives fast control of torque compared to vector control [3], [4], [5], and [6] it is rather easy to implement. Usually the DTC has been implemented using either variable switching frequency or constant switching frequency techniques. In conventional DTC [7], [8], [9] variable switching frequency hysteresis controller is applied for inverter control. It is simple and gives large benefits however;

the main drawback of this method is the wide band of the switching frequency of the inverter even when the flux and torque references are kept constant.

The three prominent multilevel inverters topologies can be used in motor drive applications. Cascaded multilevel inverters are well suited for applications where several dc power supplies could be available, such as in automotive applications. Diode-clamped and flying-capacitor multilevel structures are well suited for drives directly connected to the utility power system in the high- and medium-voltage ranges. Due to the advantage of needing only one power supply, inverters based in these topologies are very attractive for industrial Variable-Speed Drive (VSD) applications.

When diode-clamped or flying-capacitor multilevel-based inverters are used in VSD applications, the voltage across the capacitors used in these topologies could diverge from its required value [10], [11], [12], [13], [14], [15]. The control strategy used to command the multilevel inverter must take into account the charging and discharging phenomena of the capacitors.

In principle, DTC method is based on instantaneous space vector theory. By optimal selection of the space voltage vectors in each sampling period, DTC achieves effective control of the electromagnetic torque and the stator flux on the basis of the errors between their references and estimated values. It is possible to directly control the inverter states through a switching table, in order to reduce the torque and flux errors within the desired bands limits [16], [17]. The present work is based on the study of the application of DTC to the five-level inverter.

2. Proposed Five-level Inverter Topology

Important technological improvements have been achieved in the design of fast full-controlled semiconductors like IGBTs. These improvements

have allowed the increase of maximum voltage and current ratings, but an important limitation on the handled power still exists. Besides, the use of IGBTs with fast switching under high voltages may generate high dV/dt s, which may increase Electromagnetic interference and windings insulation stress. In order to

overcome these drawbacks an evolution toward new and more efficient conversion structures, such as multilevel inverters, has been observed in the field of medium voltage drive applications (up to 6.6 kV rated motors).

Table 1: Switching states of a five-level inverter

State of Switches								Output Voltage (V_{a0})
S_{a1}	S_{a2}	S_{a3}	S_{a4}	S_{a5}	S_{a6}	S_{a7}	S_{a8}	
OFF	OFF	OFF	ON	ON	ON	OFF	OFF	$-2U_0$
OFF	OFF	OFF	ON	ON	OFF	OFF	ON	$-U_0$
OFF	OFF	OFF	ON	OFF	OFF	OFF	OFF	0
OFF	OFF	ON	OFF	OFF	OFF	OFF	OFF	0
OFF	ON	ON	OFF	OFF	OFF	ON	OFF	U_0
ON	ON	ON	OFF	OFF	OFF	OFF	OFF	$2U_0$

Table 2: Five-level inverter output magnitudes of space voltages vectors

Group	Magnitude of Voltage Vectors
1	(V_0)
2	$(V_1, V_2, V_3, V_4, V_5, V_6)$
3	$(V_{44}, V_{45}, V_{46}, V_{47}, V_{48}, V_{49})$
4	$(V_{26}, V_{27}, V_{28}, V_{29}, V_{30}, V_{31})$
5	$(V_{75}, V_{76}, V_{77}, V_{78}, V_{79}, V_{80}, V_{81}, V_{82}, V_{83}, V_{84}, V_{85}, V_{86})$
6	$(V_{63}, V_{64}, V_{65}, V_{66}, V_{67}, V_{68})$
7	$(V_{118}, V_{119}, V_{120}, V_{121}, V_{122}, V_{123})$
8	$V_{106}, V_{107}, V_{108}, V_{109}, V_{110}, V_{111}, V_{112}, V_{113}, V_{114}, V_{115}, V_{116}, V_{117}),$
9	$(V_{100}, V_{101}, V_{102}, V_{103}, V_{104}, V_{105})$

Fig.1 shows the schematic diagram of Neutral Point Clamped (NPC) five-level VSI. Each phase consists of six switches, each one with its freewheeling diode in series and two other in parallel and two clamping diodes that allow the connection of the phases outputs to the middle point o. Table 1 illustrates the switching states of this inverter for one phase. Five-level NPC converter topology typically consists of four capacitors on the DC bus and five-levels of the phase voltage. Fig.1 shows a five-level NPC inverter topology in which the DC bus consists of four capacitors C_1 , C_2 , C_3 , and C_4 . For a dc bus voltage V_{dc} , the voltage across each capacitor is $V_{dc}/4$, and each device voltage stress will be limited to one capacitor voltage level $V_{dc}/4$, through clamping diodes. A five-level inverter has 125 switching states and there are 61 effective vectors. According to the magnitude of the voltage vectors, we divide them into nine (9) groups as shown in below table 2.

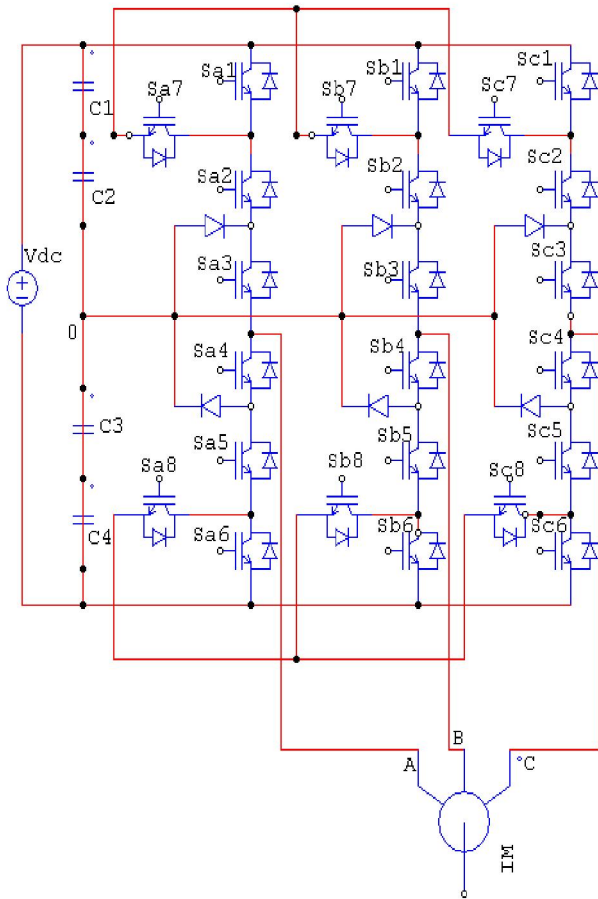


Fig.1: Proposed Five-level inverter topology

3. SVM Algorithm Implementation of Five-Level Inverter

In the case of five-level inverter, the voltage V_{dc} , in the normalized space vector representation is represented by a vector of length 4. The switching vectors located at the six vertices of the hexagon forming the periphery are same as the vectors of equivalent two-level inverter, but they have the switching states as (400), (440), (040), (044), (004), (404). The position of reference space vector $A_{00}P$ for five-level inverter is as shown in Fig.2. The first step in the proposed sector identification of this method is to determine the location of the tip of the reference space vector $A_{00}P$ from among the six regions of the equivalent two-level inverter. The region I is formed by the vertices A_{00} , A_{01} and A_{02} . The co-ordinates of the vertices are (0, 0), (4, 0) and (2, $2\sqrt{3}$) respectively as shown in Fig.2. The switching states of the vector located at A_{00} , A_{01} and A_{02} are (000, 111, 222, 333, 444), (400) and (440) respectively. The next step is to divide region I into four smaller triangular regions by applying the triangularisation algorithm and generates the co-ordinates of the new voltage space vectors and the inverter states corresponding to these new switching vectors.

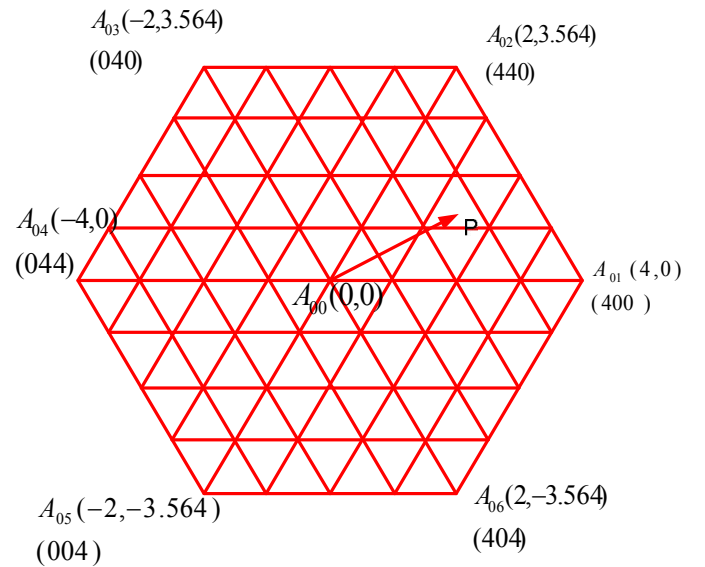


Fig.2: Space vector representation of five-level inverter

The location of the tip of the reference voltage space vector $A_{00}P$ among these four triangular regions is found by determining the region whose centroid is the closest to the tip of reference space vector. The co-

ordinates of the centroid of an equilateral triangle can be determined the average of co-ordinates of the three vertices.

The triangle with centroid closest to tip of reference space vector is $\Delta A_{11}A_{12}A_{13}$. For five-level inverter the triangularisation algorithm has to be applied once again, which generates further three new voltage space vectors and also the inverter states corresponding to these new voltage vectors, thus dividing it into four smaller triangles, the triangle enclosing the reference space vector $A_{00}P$ is $\Delta A_{23}A_{25}A_{26}$ as its centroid is the closest to tip of reference space vector. The $\Delta A_{23}A_{25}A_{26}$ corresponds to sector 27 of five-level inverter. The sector is identified and the inverter states are also generated simultaneously.

For the voltage reference vector $A_{00}P$, the sector identified is sector 27. The voltage space vector with tip located at A_{23} becomes the virtual zero vector for sector 27. The sector 27, thus, gets mapped to sector 1 of the five-level inverter. The determination of duration now reduces to that of a two-level inverter since after mapping one of the vectors of the identified sector coincides with the zero vectors. The durations of the vectors can be determined using the conventional two-level inverter.

4. Proposed Direct Torque Control using Five-level NPC Inverter fed VSI

When a five-level inverter is used to feed DTC induction motor, the number of available space voltage vectors is increased, as the number of discrete voltage levels per phase is increased. A typical block diagram of a five-level NPC inverter feeding DTC induction motor drive is shown in Fig.3. The IM control strategy will generate a space voltage vector requirement in order to keep the given external references (torque, speed or position) at their right values. The inverter control strategy must command each inverter leg with the voltage level needed to have the requested voltage vector.

In a symmetrical three-phase induction machine, the instantaneous electromagnetic torque is given by

$$T = \frac{3}{2} p \vec{i}_s \cdot j\vec{\Psi}_s \quad (1)$$

Where $\vec{\Psi}_s$ is the stator-flux-linkage vector, \vec{i}_s is the stator current vector, and the 'p' number of pole pairs.

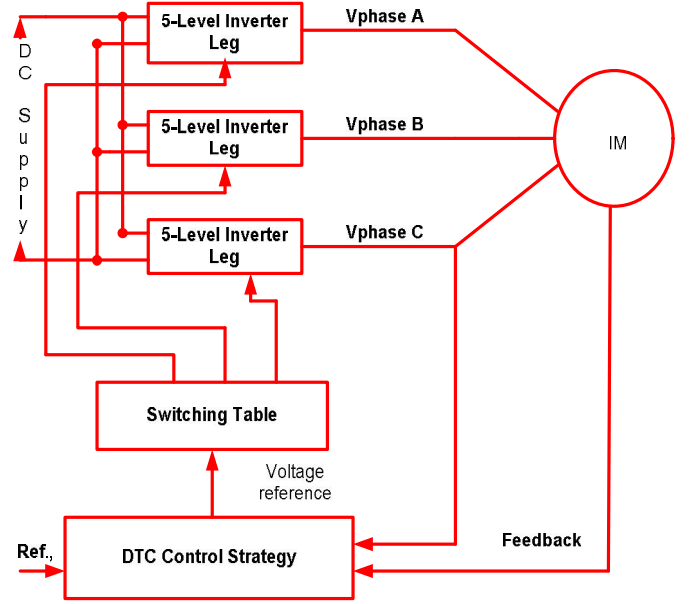


Fig.3: Proposed Block diagram of 5-level NPC inverter DTC IM drive

Both space vectors are expressed in the stationary reference frame. Another equivalent expression to calculate the electromagnetic torque, which gives an extremely clear idea of the process of controlling torque in a DTC system, is as follows

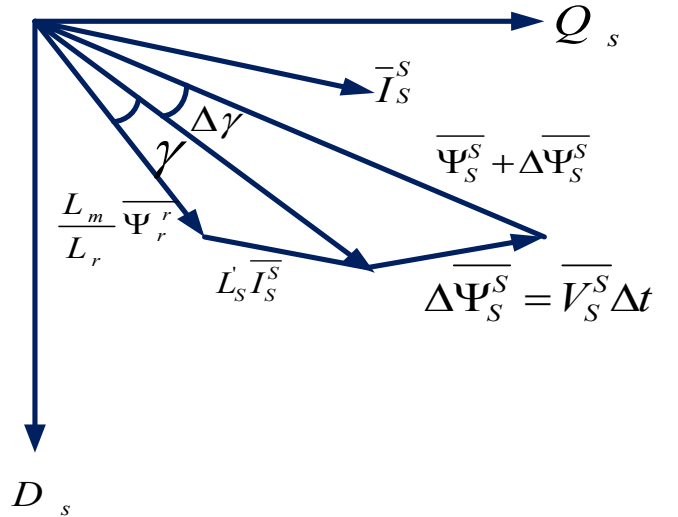


Fig.4: Induction motor flux phasor diagram

The electromagnetic torque given by equation (1) is a sinusoidal function γ of, the angle between $\vec{\Psi}_s$ and $\vec{\Psi}_r$ as shown in Fig. 4. Since the rotor flux changes

slowly, the rapid variation of stator flux space vector will produce a variation in the developed torque because of the variation of the angle γ between the two vectors:

$$\Delta T_e = \frac{3}{2} \cdot \frac{P}{2} \cdot \frac{L_m}{L_s L_r - L_m^2} [(\bar{\Psi}_s^s + \Delta \bar{\Psi}_s^s) \bar{I}_r^s] \quad (2)$$

Therefore, to obtain a good dynamic performance, an appropriate inverter voltage vectors \bar{V}_i has to be selected to obtain stronger rotation speed of The actual value of stator flux can be expressed as ω_s The actual value of stator flux can be expressed as

$$\bar{\Psi}_s^s = \int (\bar{V}_s^s - \bar{i}_s^s R_s) dt \quad (3)$$

Where \bar{V}_s^s and \bar{i}_s^s indicate the measured stator voltage and current respectively.

The electromagnetic torque is calculated by means of equation (4)

$$T_e = \frac{3}{2} \cdot P \cdot (\Psi_{ds}^s i_{qs}^s - \psi_{qs}^s i_{ds}^s) \quad (4)$$

On the other hand, the stator voltage space vector is given by

$$\bar{V}_s = R_s * \bar{i}_s + \frac{d}{dt} \bar{\Psi}_s \quad (5)$$

Where R_s is the stator resistance. If it is assumed that the stator ohmic drops can be neglected, then

$$\bar{V}_s = \frac{d\bar{\Psi}_s^s}{dt} \quad (6)$$

which simply means that the stator voltage directly defines the stator flux and, thus, the required stator flux locus will be obtained by using the appropriate inverter voltage vector. By assuming a slow motion of the rotor-flux-linkage space vector, if a stator voltage space vector is applied, which causes a quick movement of the stator flux linkage vector, then the electromagnetic torque will be increased. This is because the angle γ is increased. However, if a voltage space vector is applied which almost stop the rotation of the stator-flux-linkage space vector, then the electromagnetic torque will be decreased, because the rotor-flux-linkage vector is still moving and the angle γ decreases

Therefore the variation of the stator flux space vector due to the application of the stator voltage vector \bar{V}_s^s during a time interval of Δt can be approximated as

$$\Delta \bar{\Psi}_s^s = \bar{V}_s^s \Delta t \quad (7)$$

As in the original DTC principle [18], [19],[20] the $\alpha - \beta$ plane will be divided into several sectors. In a multilevel inverter the number of available discrete voltage vectors is more important than those obtained with a two-level inverter. Thus, the $\alpha - \beta$ plane will be divided into 12 sectors rather than six, at each one of these sectors, an appropriate voltage vector will be assigned to keep flux and torque references as needed.

For the switching vector selection, it is necessary to known the angular sector in which the actual flux is located. The actual position of the stator flux can be determined by equation (8), from the orthogonal flux components:

$$\alpha = \angle \bar{\Psi}_s^s = \tan^{-1} \left(\frac{\Psi_{qs}^s}{\Psi_{ds}^s} \right) \quad (8)$$

The selection of the appropriate voltage vector is based on the switching table given in Table 3. The input quantities are the stator flux sector and the outputs of the two hysteresis comparators. Assuming the stator flux vector lying in sector 1 of the $\alpha - \beta$ plane, the voltage vectors used by DTC technique are shown in Fig. 5.

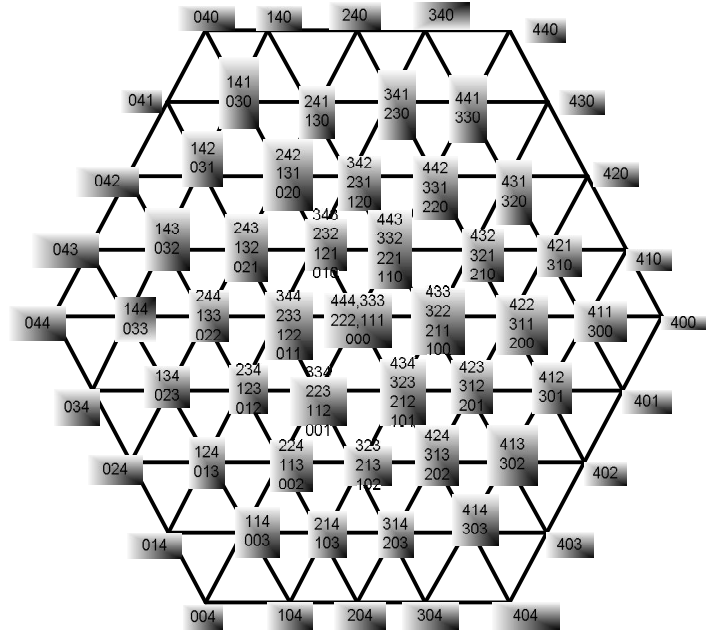


Fig.5: Space voltage vectors used in a five-level inverter fed DTC scheme

Table 3: Proposed switching table for 5-Level NPC Inverter fed DTC IM drive

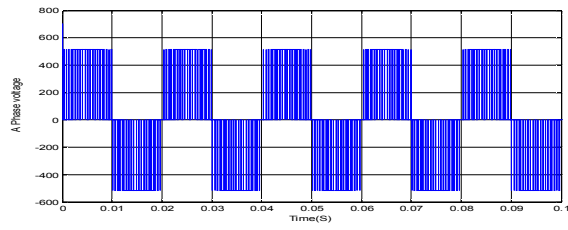
		Sectors											
C_Φ	C_r	1	2	3	4	5	6	7	8	9	10	11	12
+1	+4	107	101	109	102	111	103	113	104	115	105	117	100
	+3	76	64	78	65	80	66	82	67	84	68	86	63
	+2	118	27	119	28	120	29	121	30	122	31	123	26
	+1	44	2	45	3	46	4	47	5	48	6	49	1
	0	Zero Vector											
	-1	49	1	44	2	45	3	46	4	47	5	48	6
	-2	123	26	118	27	119	28	120	29	121	30	122	31
	-3	68	85	63	75	64	77	65	79	66	81	67	83
	-4	105	116	100	106	101	108	102	110	103	112	104	114
	+4	102	110	103	112	104	114	105	116	100	106	101	108
-1	+3	65	79	66	81	67	83	68	85	63	75	64	77
	+2	28	120	29	121	30	122	31	123	26	118	27	119
	+1	3	46	4	47	5	48	6	49	1	44	2	45
	0	Zero Vector											
	-1	5	48	6	49	1	44	2	45	3	46	4	47
	-2	30	122	31	123	26	118	27	119	28	120	29	121
	-3	67	83	68	85	63	75	64	77	65	79	66	81
	-4	104	114	105	116	100	106	101	108	102	110	103	112
	+4	109	102	111	103	113	104	115	105	117	100	107	101
	+3	78	65	80	66	82	67	84	68	86	63	76	64
0	+2	119	28	120	29	121	30	122	31	123	26	118	27
	+1	45	3	46	4	47	5	48	6	49	1	44	2
	0	Zero Vector											
	-1	48	6	49	1	44	2	45	3	46	4	47	5
	-2	122	31	123	26	118	27	119	28	120	29	121	30
	-3	67	83	68	85	63	75	64	77	65	79	66	81
	-4	104	114	105	116	100	106	101	108	102	110	103	112

The flux control is made by classical two-level hysteresis controller, so a high level performance torque control is required, and the torque is controlled by an hysteresis controller built with four lower bounds and four upper known bounds.

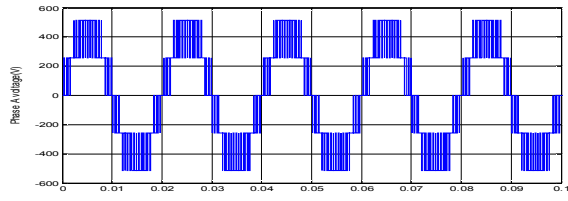
Positive torque is applied for acceleration and negative torque is applied for retardation. When controlled torque reaches the positive lower hysteresis band, the full voltage vector is replaced with half voltage. If torque increases beyond the positive upper torque band, the zero voltage vectors are applied to decrease the developed torque. For reverse rotation, in the same way, retarding voltage vectors are applied.

5. Simulation Results and Discussion

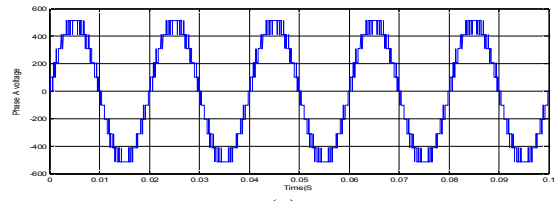
To verify the proposed scheme, simulation studies have been carried out for two-level, three-level and five-level NPC inverter fed DTC IM Drive. The simulation parameters of induction motor used in this method are given as follows: $R_s=4.85\Omega$, $R_r=3.805\Omega$, $L_s=274\text{mH}$, $L_r=274\text{mH}$, $L_m=258\text{mH}$, $p=2$, $J=31\text{g.m}^2$, $V=220\text{V}$, power=1.5kW and speed=1420rpm. All simulations have a sample time for the control loop of 100 μs ; the voltage of the DC bus is 514V. The amplitudes of hysteresis band are fixed as follows: $\Delta\Phi_s=3\%$, $\Delta\Gamma_1=0.3\%$, $\Delta\Gamma_2=0.7\%$, $\Delta\Gamma_3=1.3\%$, $\Delta\Gamma_4=3\%$ for five-level DTC strategy. To show the effectiveness of the DTC with five-level inverters with SVPWM switching technique a simulation work has been carried out on induction motor.



(a)

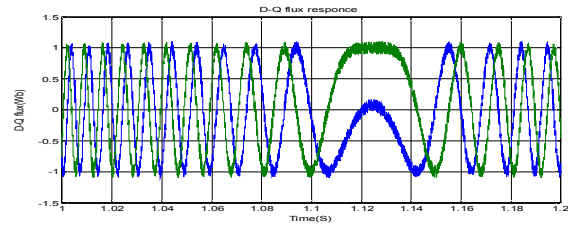


(b)

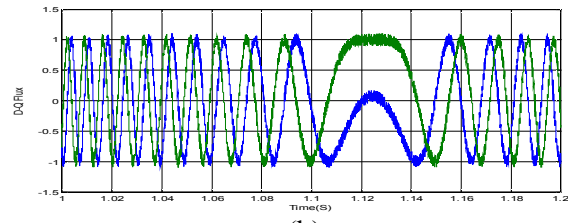


(c)

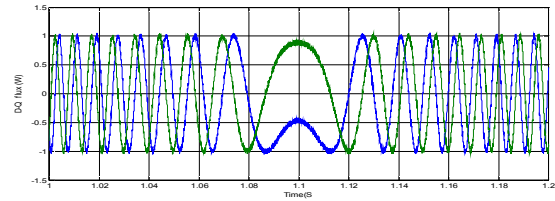
Fig.6: a-c: Line Voltages of 2,3and 5-level inverter



(a)

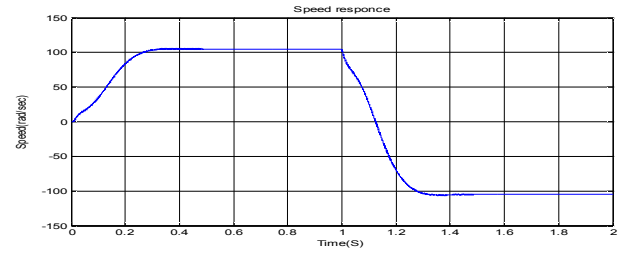


(b)

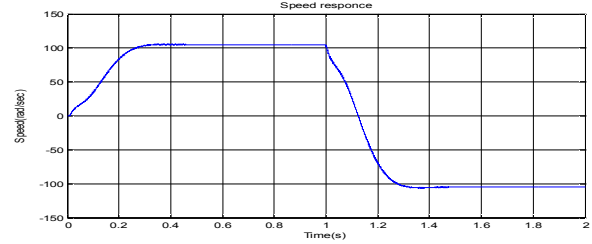


(c)

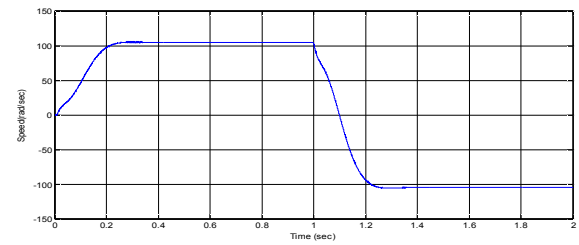
Fig.7:a-c D-Q axis flux of Two-level, Three-level and Five-level inverter fed DTC IM drive, current reversal at 1sec



(a)

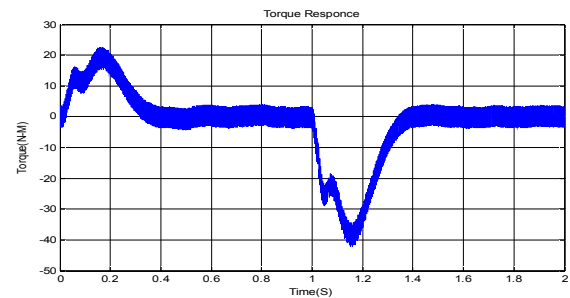


(b)

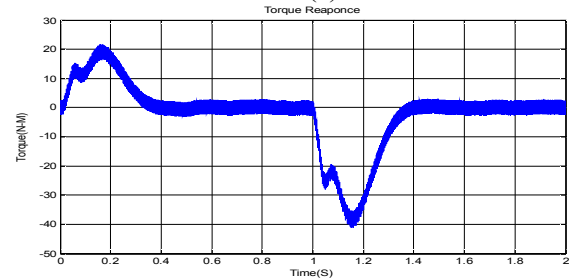


(c)

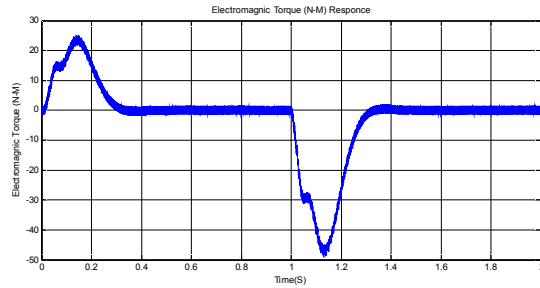
Fig.8: a-c Speed response of Two-level, Three-level and Five-level inverter fed DTC IM drive, current reversal at 1sec.



(a)



(b)



(c)

Fig.9: a-c Torque response of Two-level, Three-level and Five-level inverter fed DTC IM drive, current reversal at 1sec.

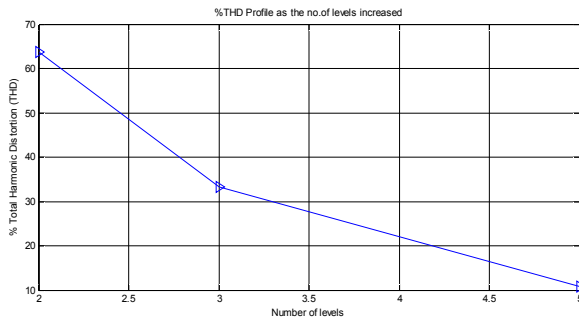


Fig.10: %THD profile as the number of levels increase

The stator line voltages of two-level, three-level and five-level inverter system are illustrated in fig.6. In fig.7 D-Q axis flux response of the two-level, three-level and five-level inverters are compared. It is seen that the performance of the five-level inverter fed DTC IM drive has lower ripple, so the proposed system is superior to control the flux with reduced ripple content. Fig. 8 illustrate the speed response of two-level, three-level and five-level inverter fed DTC IM drive, from simulation results proposed system has fast dynamic speed response. Fig.9 shows the torque response of two-level, three-level and five-level inverter fed DTC IM drive when current reversal at 1sec; demonstrates the developed DTC's achieved high dynamic performance in response to changes in demand torque. Fig.10 shows the decrease of percentage of Total Harmonic Distortion (%THD) in the motor line voltage as the number of levels increased. This result in smooth running of motor and the performance of the motor can be improved. From the above discussion, the proposed DTC IM drive system behavior is optimum, even in extreme conditions like the reverse speed reference with

nominal load torque applied. Reduction in ripple is observed in both electromagnetic torque and flux is due to the use of hysteresis controllers.

6. Conclusion

A multilevel inverter based DTC fed induction motor drive using space vector modulation is presented. The proposed DTC IM drive scheme is capable for enough degrees of freedom to control both electromagnetic torque and stator flux with very low ripple.

Even with at the output voltages with extremely low distortion and lower dv/dt they can operate with a lower switching frequency. As the number of levels increased the %THD in the motor line voltage decreased. As the number of levels increased the torque ripple is reduced to minimum and the stator flux ripple is also minimized. From this analysis high dynamic performance, good stability and precision are achieved.

References

1. M. F. Escalante, J-C. Vannier and A. Arzandé. *Flying Capacitor Multilevel Inverters and DTC Motor Drive Applications*. IEEE Trans. On Industrial Electronics, vol. 49, (No.4), pp. 809-815, 2002.
2. J. Rodriguez, J-S Lai and F. Z. Peng. *Multilevel Inverters: A survey of topologies, controls, and applications*. IEEE Trans. On Industrial Electronics, vol. 49, (No.4), 2002.
3. Madhav D. Manjrekar and Thomas A. Lipo, *A Hybrid Multilevel Inverter Topology for Drive Application*, in Proceedings of the 1998 IEEE – APEC Conference, pp.523-529
4. A.Rufer, M.Veenstra and K.Gopakumar, *Asymmetric Multilevel Converter for High Resolution Voltage Phasor Generation*, in Proceedings of the 1999 EPE Conference, pp.P1-P10.
5. S. Busquets-Monge, S. Alepuz, J. Bordonau, and J. Peracaula, *Voltage balancing control of diode-clamped multilevel converters with passive front-ends*, IEEE Trans. Power Electron., vol. 23, no. 4, pp. 1751–1758, Jul. 2008.
6. Y. Zhang and Z. Zhao, *Study on capacitor voltage balance for multi-level inverter based on a fast SVM algorithm*. Proc. CSEE, vol. 26, no. 18, pp. 71–76, 2006, (in Chinese).
7. Dalessandro, S. D. Round, and J. W. Kolar, *Center-point voltage balancing of hysteresis current controlled three-level pwm rectifiers*, IEEE Trans. Power Electron., vol. 23, no. 5, pp. 2477–2488, Sep. 2008.
8. A. Nabae, I. Takahashi, and H. Akagi, *A new neutral-point clamped PWM inverter*, IEEE Trans. Ind. Appl., vol. IA-17, no. 5, pp. 518–523, Sep. 1981

9. J.-S. Lai and F. Z. Peng, *Multilevel converters—A new breed of power converters*, *IEEE Trans. Ind. Applicat.*, vol. 32, pp. 509–517, May/June 1996.
10. B. McGrath, D. Holmes, T. Lipo, *Optimized Space Vector switching sequences for multilevel inverters*, *IEEE Transactions on Power Electronics*, 2003, 18(6): 1293–1301.
11. Z. Pan, F. Peng, et al. *Voltage balancing control of diode-clamped multilevel inverter system*, *IEEE Transactions on Industry Applications*, 2005, 41(6): 1698–1706.
12. J. Pou, D. Boroyevich, R. Pindado, *New Feed forward Space-Vector PWM Method to Obtain Balanced AC Output Voltages in a Three-Level Neutral-Point-Clamped Converter*, *IEEE Transactions on Industrial Electronics*, 2002, 49(5): 1026–1034.
13. J. Rodriguez, J. Lai, F. Peng, *Multilevel Inverters: A Survey of Topologies, Controls and Applications*, *IEEE-IETrans. On Industrial Electronics*, 2002, 49(4): 724–738.
14. P. Satish Kumar, J. Amarnath and S.V.L. Narasimham, *An Analytical Space-Vector PWM Method for Multi-Level Inverter Based on Two-Level Inverter*, *International Review on Modelling and Simulations (IREMOS)*, Vol. 03, n.01, pp. 1-9, February 2010.
15. I. Takahashi and T. Nogushi, *A new quick-response and high efficiency control strategy of induction motor*, *IEEE Trans. On. IA*, vol. 22, (No.5), pp. 820-827, 1986.
16. G. Buja, D. Casadei and G. Serra, *Direct torque control of induction motor drives*, *Proc. IEEE International Symposium on Industrial Electronics*, vol. 1, pp. TU2-TU8, 1997.
17. P. Vas, *Sensor less Vector and Direct Torque Control*. Oxford, U.K.: Oxford Univ. Press, 1998.
18. D. Casadei, G. Grandi, G. Serra and A. Tani, *Switching strategies in direct torque control of induction machines*, *ICEM 94*, Vol. 2, pp. 204-209, 1994.
19. I. Messaif, E.M. Berkouk, N. Saadia and A. Talha, *Application of Direct Torque Control Scheme for Induction Motor*, *International AMSE Conference MS'05*, 2005.
20. Messaif, E.M. Berkouk, N. Saadia, *An Improved DTC strategy for induction machine control fed by a multilevel voltage source inverter*, *IEEE International Conference on Electronics, Circuits and Systems*, Morocco.